Journal of Education and Science (ISSN 1812-125X)

Optimization of Radar Rainfall Estimation in Yogyakarta using a Time Correction Approach and DEM-Based Height Selection

F. E. Penalun [1*], A. S. Syahab [2]

[1,2] Climatology Station of Yogyakarta, Indonesian Agency for Meteorology Climatology and Geophysics, Indonesia

Article information

Article history:
Received: January 05, 2026
Revised: March 26, 2026
Accepted: May 01, 2025
Available online: July 01, 2026

Keywords:
Weather Radar
QPE
Phase Locking
Marshall-Palmer
Optimal AGL

Correspondence:
Ferdinandus Edwin Penalun
edwinpenalun@gmail.com

Abstract

The accuracy of quantitative precipitation estimation (QPE) using radar is often hindered by uncertainties in the vertical reflectivity profile and time discrepancies with surface measurements. This study aims to determine the most appropriate sampling height above ground level (AGL) and align the time lag between weather radar data and tipping bucket rain gauges. The methods used include rigorous filtering of multi-volume raw data to reduce bias, followed by retrieving converted reflectivity using the Marshall-Palmer Z–R relationship. Phase locking analysis shows that a 10-minute backward time shift (Time Shift -1) yields the highest correlation, reflecting the rainfall duration and sensor delay. Vertical evaluation reveals a compromise between accuracy and stability at an altitude of 600 m, where the lowest average RMSE (0.779 mm) was obtained. This altitude is optimal for low-lying areas, despite a high level of instability (standard deviation of 0.493) due to interference in mountainous areas. Meanwhile, an altitude of 1400 m demonstrates the best data stability (standard deviation of 0.185). This study recommends applying a -10-minute time correction and using data at altitudes above 1200 m as the optimum zone to reduce topographic distortion in regions with dynamic contours.

DOI:10.33899/jes.v35i3.60402,

1. Introduction

Radar does not measure rainfall directly but calculates rainfall rates based on the number and size of raindrops. This indirect measurement method leads to a high degree of uncertainty in rainfall estimation [1], [2]. However, estimating rainfall from reflectivity values at specific heights above the surface has shown a strong correlation when compared to ground-based measurements [3], [4]. Weather radar remains a vital instrument in rainfall monitoring due to its ability to provide data with high spatial and temporal resolution [5]. Nevertheless, to ensure radar data accurately represent surface rainfall, field calibration or validation is essential. Without calibration, rainfall estimation results may exhibit significant deviations, rendering them less representative of actual ground conditions [6]. Several factors pose challenges in performing Quantitative Precipitation Estimation (QPE) based on radar. These include phenomena such as bright bands, beam overshooting, signal attenuation, partial beam blockage (PBB), and ground clutter, all of which introduce bias into the received reflectivity [7]. Significant bias often arises from the bright band (BB) phenomenon in the melting layer, where reflectivity values become artificially high. This potentially leads to overestimation when compared with surface rainfall [8], [9]. Additionally, topography can obstruct the radar beam during scanning, causing the radar to capture backscatter from terrestrial obstacles rather than precipitation. This issue is prevalent in mountainous regions and densely populated urban areas [10].

Numerous studies have addressed these challenges, with rapid developments in estimation techniques to account for spatial, temporal, and atmospheric physical processes. Several approaches have been adopted, such as considering the total number concentration (N^T) and median volume diameter (D_o), which have proven effective in explaining the variability of the

Z–R relationship. Analysis using disdrometer data in Africa demonstrates that combining (N^T) and (D_o) improves radar rainfall estimation accuracy [11]. Another study compared three correlations—Marshall–Palmer, Muchnik, and Joss—using CAPPI (Constant Altitude Plan Position Indicator) at heights of 1 km and 1.5 km AGL, calibrated with rain gauge data. The results indicated that the Marshall–Palmer relationship at 1.5 km AGL produced the smallest deviation and the strongest correlation with gauge data [7]. Furthermore, a study conducted in the same area as this research highlights that elevation-dependent corrections, derived from the Log (G/R) relationship relative to gauge elevation, contribute to reducing estimation errors, particularly in light rain cases. These studies provide a fundamental basis for the research presented in this paper. The primary focus of this research is to analyze and identify the optimal sampling height within the lower atmospheric layer that is most representative of surface rainfall. The goal is to select a height close to the surface that avoids the bright band zone, which typically forms at an altitude of 4–5 km above mean sea level (AMSL) in tropical regions [12]. The altitudes evaluated in this study are 600, 800, 1000, 1200, 1400, and 1600 m above ground level (AGL), using radar products that follow the topographic contours of the study area. Additionally, this selection considers that cloud observations in the research location, specifically the cloud base height (CBH), frequently occur at altitudes of 800 to 1000 meters AMSL [13]. In addition to height selection, this study examines the temporal bias between radar scans and tipping bucket measurements. This analysis aims to achieve temporal synchronization between radar observations and rain gauges. Correcting this lag is crucial, primarily due to the physical time required for raindrops to descend from the radar sampling height to the ground [14].

2. MATERIALS AND METHODS

a. Data

The weather radar utilized in this study is located in Yogyakarta at an altitude of 182 meters AMSL. Operated by the Meteorology, Climatology, and Geophysics Agency (BMKG), it serves as the primary instrument for regional hydrometeorological monitoring. This C-band radar operates at a frequency of 5.64 GHz with a single-polarization system. Key technical specifications include a pulse width of 0.5–2.0 μs, a Pulse Repetition Frequency (PRF) of 250–2000 Hz, an angular resolution of <1°, and an antenna rotation speed of 36°/s. The radar employs a scanning strategy consisting of 10 elevation angles to generate a single volume of data within a duration of 228.5 seconds, with a temporal resolution of 10 minutes.

Various external factors can cause uneven signal distribution, including attenuation, hydrometeor diversity, topographic contours, propagation anomalies, and noise correction issues, which result in the degradation of measurement accuracy [15]. The Level-2 radar products used in this study are reflectivity (Z) values derived from raw volumetric data that have undergone the radar system's built-in filtering. This internal filtering aims to mitigate clutter and non-meteorological interference, ensuring the data is more representative of actual atmospheric phenomena [16]. The efficacy of this built-in filtering is illustrated in Figure 1, which displays the clutter presence before filtering, and Figure 2, which shows the post-filtering results. Generally, this process yields cleaner reflectivity data suitable for meteorological analysis. However, previous studies indicate that while filtering significantly improves data quality, residual noise and artifacts may persist [17]

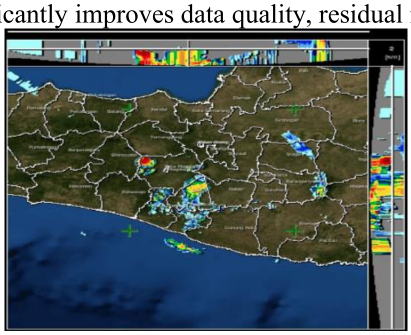

Figure 1. Radar image before filtering

Figure 2. Radar image after filtering

Subsequently, a product adjusted to topographic contours was generated according to specific AGL height settings (terrain-adjusted surface projection). Unlike the conventional Constant Altitude Plan Position Indicator (CAPPI), which presents data at a fixed altitude relative to the radar site [18], this product dynamically adapts to terrain elevation based on a Digital Elevation Model (DEM), making it significantly more representative of complex topography.

In this study, radar data extraction was performed using the wradlib library [19]. Sample points, spatially matched to the geographic coordinates (latitude and longitude) of the rain gauge positions, served as the basis for validation and calibration. The ground reference data were obtained from 15 observation stations distributed across the Special Region of Yogyakarta, covering the period of September, October, and November 2025, as illustrated in Figure 3.

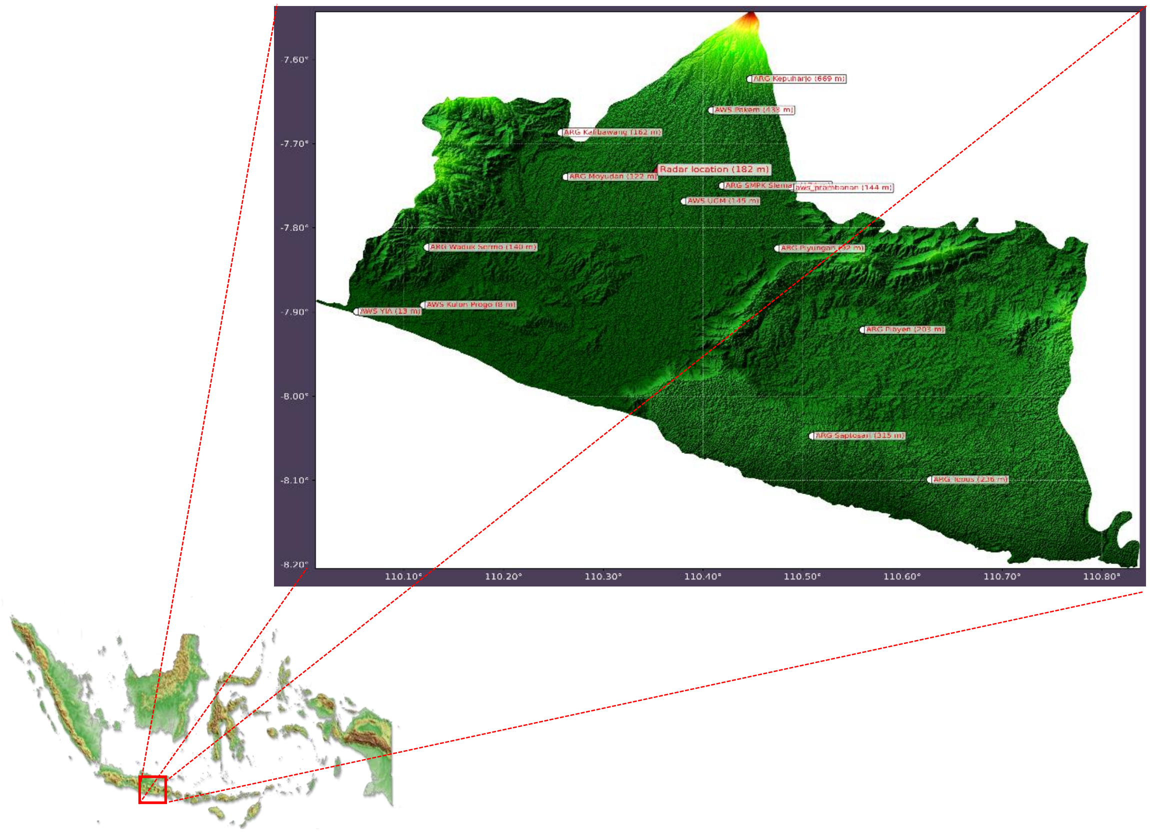

Figure 3. Location of surface observation data

b. Method

This research method involves several main stages, beginning with the acquisition of weather radar data and surface rainfall data (rain gauge). The next stage is the extraction of radar data to obtain reflectivity values at various heights. After that, preprocessing is carried out on the radar and rainfall data. Both types of data then undergo a data matching process to synchronize the time references between radar and surface observations. The phase locking technique is then tested to synchronize the data and identify the time lag with the best representation. The final stage of the research involves analyzing the determination of the optimal sampling height to produce the best rainfall estimation accuracy.

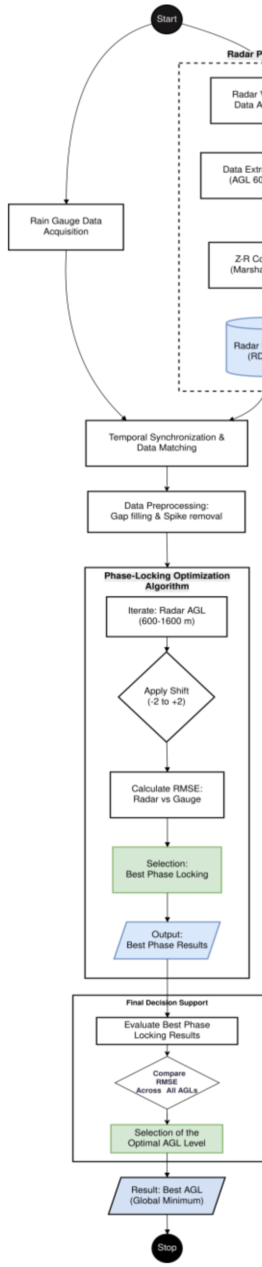

Figure 4. Research Methodology

Figure 4 shows all the stages of this research process, which will be explained in the following points.

3. Radar data extraction

The wradlib library was utilized to process raw multivolume radar data, extracting reflectivity, elevation, and azimuth information, along with metadata such as radar location (longitude, latitude, altitude) to serve as spatial references [20], [21]. The steps involved creating a horizontal grid based on geographic coordinates (longitude-latitude) with a resolution of 500 meters. To determine the range, a radius of 75 km from the radar location was used, which covered the entire research area. For DEM data, reprojection into the radar grid is performed using bilinear interpolation to obtain values from the reflectivity data at the previously set height to calculate the height from the ground surface at each reflectivity on the radar grid.

Valid reflectivity values are used to form a grid that follows the topography at each predetermined AGL level. The values taken are the maximum values within a 2 km radius above the rain gauge point. These reflectivity values are then converted into rainfall estimates using the Marshall–Palmer Z–R relationship [22], resulting in rainfall rates in mm/hour. To ensure comparability with surface observation data, which are recorded as 10-minute accumulations, the hourly rainfall rate must be converted. Assuming constant rainfall intensity during the observation interval, the hourly rate is divided by 6, as formulated in Equation (1):

$$Z = 200R_{hour}^{1.}6 \Rightarrow R_{hour} = (Z/200)^{(1/1.6)}$$

$$R_{10} = 1/6(Z/200)^{(1/1.6)} \quad (1)$$

R = Estimated rainfall rate (mm within a 10-minute range)

Z = Reflectivity value

4. Preprocessing Rain Data

Rain data was collected from 15 rain gauge stations with a tipping bucket type and a resolution of 0.2 mm. After the data was collected, the first step was to fill in the missing data using the moving average method. This method estimates the value at the missing data point for a very short interval (for example, one or two missing data points). The choice in this study is very limited to only one empty data interval. If the empty data interval is too wide, this method can cause large estimation errors. This is because this method tends to have a linear and constant pattern, unlike the characteristics of rainfall, which are very dynamic and non-linear [23]. The moving average algorithm is shown in equation 2.

$$x(t) = \frac{1}{N}\sum_{i=0}^{n-1} x(t-i) \quad (2)$$

x(t) = rainfall value at time t

N = average window length (e.g., 3–5 intervals)

The next Quality Control (QC) procedure, spike filtering, aims to eliminate extreme data spikes (outliers) that have the potential to reduce the accuracy of rainfall estimates. The process of detecting and correcting anomalies in rainfall data is a mandatory step before entering the Z–R calibration process [24].

Tipping-bucket rain gauges have the potential to cause mechanical errors that can produce spurious values or sharp data spikes. Such errors are often undetectable in standard hourly QC procedures because they have accumulated. Instrument disturbances, such as electronic interference, wind vibrations, or insect blockages, can cause measurement errors [25]. The application of conventional temporal filter methods risks deleting the original rainfall data. Therefore, this study developed a QC mechanism that involves radar data as a reference for event verification.

The logic for detecting using cross-validation between these two data sets aims to obtain better performance in removing anomalous or false data [26], [27]. If the rain gauge records rainfall, while the radar data shows a low reflectivity value <15 dBZ within a fairly wide time range of ± 30 minutes (±3 data intervals), then the rain gauge record is classified as a spike or instrument error.

5. Time Shift Analysis using Phase Locking Time

Synchronization between radar data converted from radar reflectivity using the Marshall–Palmer empirical relationship and rain gauge data is matched based on the same timestamp between the two. Then, they are combined into a single dataset of radar and rain gauge data with temporal alignment between the two instruments. This data matching process is useful for conducting Time Lag Analysis between radar observation data and surface rainfall data. For testing, the smallest and most stable error value is considered so that both data sources truly reflect rainfall events at the same time [28]. The time lag range is tested up to 20 minutes backward and forward, or in other words, up to two forward and backward data intervals.

When applying this discrete time method with a selected range between –2 and +2 data intervals (–20 to +20 minutes), the radar and rainfall data in this study had the same 10-minute interval. Root Mean Square Error (RMSE) was calculated at all heights from 600 to 1600 meters for five scenarios, namely –2, -1, 0, 1, and 2. The lowest RMSE result was selected as the best shift, which indicated the best phase between the two data sets.

To interpret this, negative values (-1, -2) indicate that radar detection precedes surface rainfall, while a value of zero (0) indicates that both instruments are synchronized or that there is no time lag. Positive values (+1, +2) indicate that surface rainfall precedes rainfall detected on the radar. This step aims to ensure that the comparison between the radar and rain gauge is not only consistent in pattern but also ensures the accuracy of the values.

6. Recommended radar data height to be used

The determination of the optimal radar sampling height based on AGL is carried out through statistical analysis. This stage aims to determine the best atmospheric layer for future radar operations. The process is carried out after temporal synchronization (Phase Locking) to mitigate the time lag between radar data and rain gauges. Once the time dimension is synchronized, the evaluation continues by calculating the Root Mean Square Error (RMSE) value of the reflectivity-rainfall relationship (Z-R) at an altitude range of 600 to 1600 meters. This analysis considers not only absolute accuracy but also data stability against topographic variability mapped through DEM. The elevation layer that produces the best compromise between minimum error and spatial consistency is then recommended as the standard parameter for operational Quantitative Precipitation Estimation (QPE) input.

7. Results and Discussion

A. Results of data processing in the preprocessing stage

In the data preprocessing stage, the moving average method was used, which aimed only to fill in the empty data in one gap. The Kalibawang, Piyungan, and Moyudan stations were the three locations with the most assimilated data. This indicates that the raw data from these three stations is intermittent (discontinuous). In contrast, data from the YIA, Saptosari, and Playen locations are relatively more continuous, as seen from the smaller increase in the amount of filled data. The total amount of filled data initially amounted to 49,587 and became 52,567 with the addition of 2,980 data entries.

In the process of removing anomalous data using cross-validation between the two observations, the amount of data deleted reached 1,302 anomalous/spike data from the total data. The visualization of the data filling results and data changes in the anomaly data deletion process is shown in Figure 5.

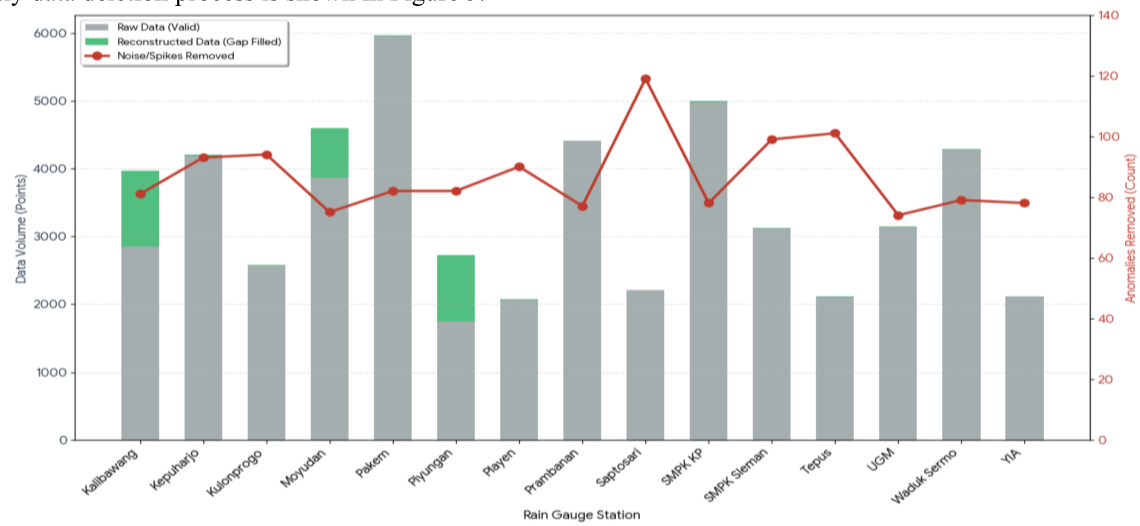

Figure 5. Gap filling and Spike removal

B. Determination of phase locking time optimization.

The most dominant time correction found was a 10-minute delay (lag -1). This lag occurs because when the radar scans water droplets in the atmosphere, the droplets need time to fall to the tipping bucket (fall speed). The tipping bucket also needs time to collect water to reach its capacity (0.2 mm resolution) before finally tipping and recording the data. Therefore, it is natural for the radar to detect rain earlier than the tipping bucket gauge.

At the YIA station, for example, rain was recorded earlier in the gauge, mostly at lag +1. This can be influenced by coastal effects, where rain often falls from low clouds (shallow convection) that escape the radar scan at certain altitudes. At Sermo Reservoir, the shift varies considerably but is predominantly without lag time (zero lag). Considering that 63 critical phase tests were selected, lag time –1 was used for subsequent data processing. The distribution of time shifts at all stations can be seen in Figure 6.

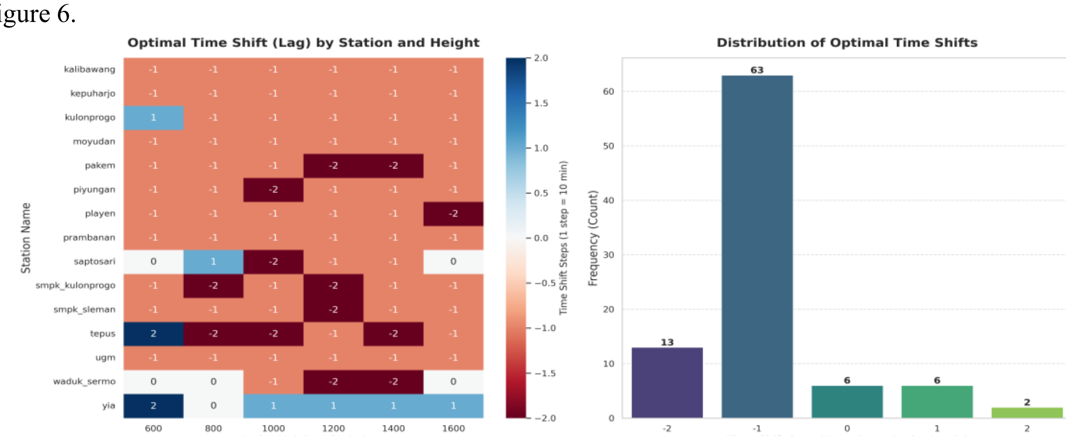

Figure 6. Optimal time shift between radar rainfall data and surface rainfall

In the future, this research will be useful for standardization, facilitating data management, and ensuring feature consistency, which are key prerequisites in the development of statistical QPE analysis and artificial intelligence-based models.

C. Optimal Height Evaluation: The Accuracy vs. Stability Dilemma

Once the time dimension was synchronized, the analysis shifted to determining the atmospheric layer (sampling layer) that is most representative of the radar data extraction results. The main challenge at this stage was to balance two conflicting metrics: Absolute Accuracy (which excels at low altitudes) and Data Stability (which excels at medium-high altitudes).

Statistical calculations show that an altitude of 600 meters generally produces the lowest average RMSE value of 0.779 mm. Theoretically, closer proximity to the surface reduces distortion due to altitude, provided that the data passed through the radar system's filtering maintains good quality. However, a closer examination of the Kepuharjo area—which has the highest elevation among all rain gauge locations—reveals the largest error of 2.30 mm. Comprehensive information can be seen in Figures 7 and 8.

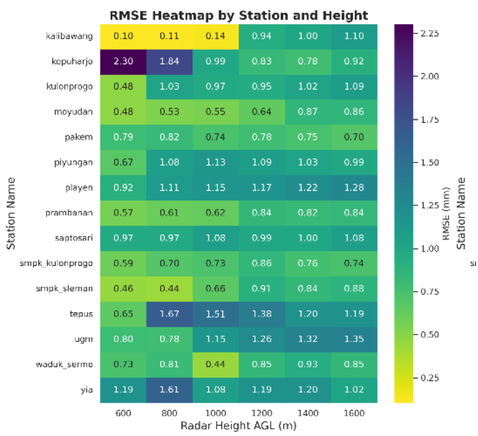

Figure 7. Comparison of RMSE for each location by elevation

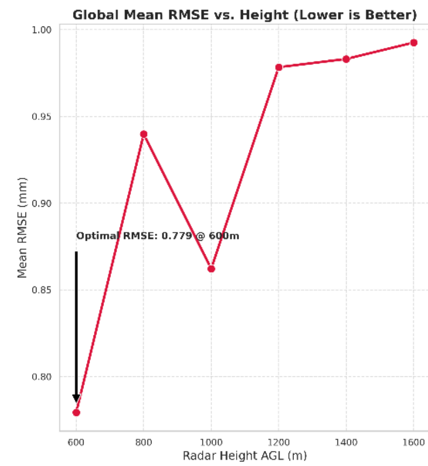

Figure 8. Average RMSE of all locations per elevation

The main cause is surface noise clutter. Radar waves are very susceptible to colliding with surface objects such as tall buildings, hills, or trees. The reflection of these objects creates false images, leading to errors in validation [29]. As a result, although accurate at some ideal points, this altitude is quite risky. Similar problems are still detected at an altitude of 800 meters and begin to decrease at an altitude of 1000 meters. This can be seen in Figures 9 and 10.

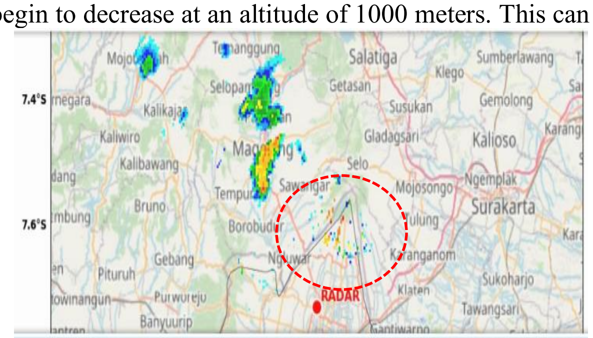

Figure 9. Height of 800 meters AGL

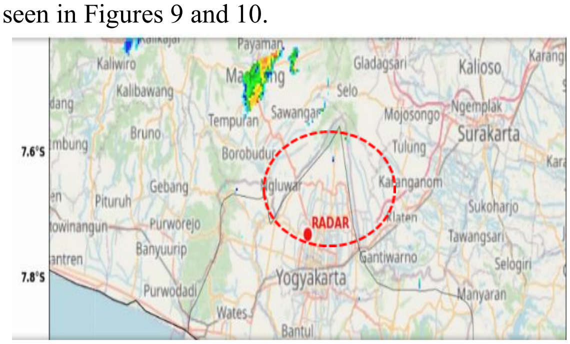

Figure 10. Height of 1000 meters AGL

pattern of very high standard deviation at low altitudes in the range of 600–800 meters (~0.47–0.49 mm), compared to higher altitudes, indicates that the data quality is highly inconsistent. Data at heights from 1200 to 1600 meters tends to have lower deviations, meaning that the error values produced are more homogeneous and stable, as shown in Table 1.

Table 1. Standard Deviation Based on Height

Height (AGL)	Std Dev RMSE (Stability)	Status
600 m	0.493	Least Stable (Very high error variation between stations)
800 m	0.476	Unstable
1000 m	0.35	Fairly Stable
1200 m	0.201	Very Stable
1400 m	0.185	Most Stable (Data quality is uniform across all stations)
1600 m	0.191	Very Stable

Analysis at an altitude of 1400 meters above ground level shows the most significant data stability, with results showing a decrease in standard deviation of up to 0.185 mm, which is much more stable than at 600 meters. These results confirm that the altitude of the rain gauge station is a critical variable in the QPE calibration process. If radar data is taken at a low altitude above ground level, rain gauges located in highlands or mountainous areas will be highly susceptible to signal distortion due to ground clutter. Conversely, by increasing the radar sampling level, topographic interference can be avoided. Therefore, this study proposes the use of data at altitudes above 1200 meters, especially for rainfall intensity in highlands or mountainous areas, as an optimal zone that is relatively resistant to contour effects.

For areas with gentle topography and minimal orographic obstruction, such as coastal areas, data collection at low altitudes (e.g., 600 m) is recommended as it yields optimal results. This is evidenced by the low RMSE values in this zone. Increasing the radar sampling elevation tends to increase the error level because, at greater distances from the surface, atmospheric physical processes introduce discrepancies in rainfall estimation. In contrast, mountainous areas show the opposite trend, where lower sampling heights increase the error level. This phenomenon is clearly visualized in Figure 11; highland stations such as AWS Pakem and ARG Kepuharjo show a decrease in error when the sampling height increases from 600 m to 1400 m, whereas at other stations, the error generally tends to increase.

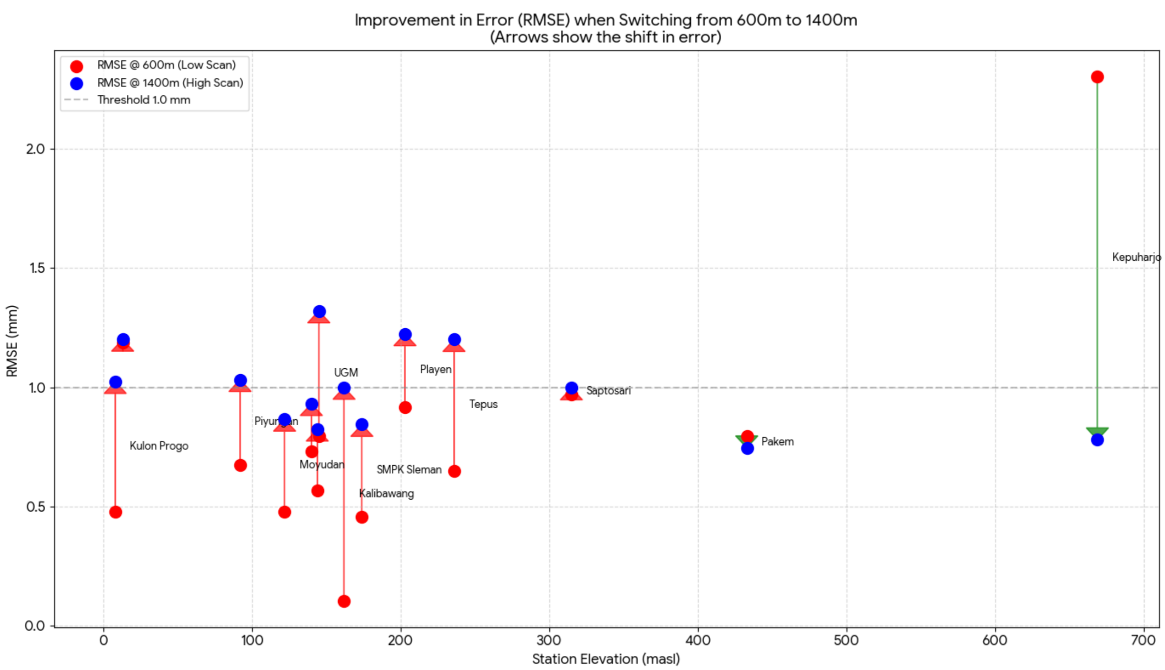

Figure 11. Variation of RMSE values across sampling heights from 600 m to 1400 m

8. Conclusion

The results of this study indicate that data pre-processing is a crucial stage in calibration and quantitative precipitation estimation (QPE). Multivolume raw data must undergo a rigorous filtering process to minimize bias and noise, which significantly determines the validity of the final QPE results. This calibration effort poses a challenge, especially in areas with dynamic contour complexity.

Technical constraints also arise due to the time lag caused by atmospheric physical processes, namely, the time required for raindrops to fall from the radar sampling height to be measured by a rain gauge. This study found that a time lag correction of a 10-minute backward shift (Time Shift -1) proved to provide the highest correlation at the majority of stations. This confirms the physical duration of rainfall and the limitations of the 0.2 mm resolution tipping bucket sensor.

An evaluation of altitude variations shows that radar data collection at low altitudes (600 meters AGL) provides the lowest error for lowland areas. However, this layer exhibits a high level of error and variability in mountainous areas (such as the slopes of Mount Merapi). Therefore, the proposed use of a single height of 600 meters is not recommended for areas with dynamic contours, except in regions with gentle topography and minimal orographic obstacles.

Conversely, analysis at an altitude of 1400 meters AGL has been proven to mitigate low-layer noise, resulting in consistent data quality in both mountainous and coastal areas. Specifically, the altitude range of 1200–1600 meters represents the layer that produces homogeneous errors. Thus, this study recommends the use of data at altitudes above 1200 meters as the optimal zone that is relatively resistant to contour effects.

9. Acknowledgments

We wish to convey our profound appreciation and heartfelt thanks to anyone who contributed to the completion of this research, especially to the Climatology Station of Yogyakarta, the Indonesian Agency for Meteorology, Climatology, and Geophysics, for the facilities that support this research.

10. Conflicts of interest

The authors report no conflicts of interest regarding this study.

11. Funding

The authors affirm that none of the work described in this publication was influenced by any known competing financial interests .

REFERENCES

[1] P. Jordan, A. Seed, and G. Austin, “Sampling errors in radar estimates of rainfall,” *Journal of Geophysical Research Atmospheres*, vol. 105, no. D2, pp. 2247–2257, 2000, doi: 10.1029/1999JD900130.

[2] T. Y. Ojebisi, J. S. Ojo, E. O. Olurotimi, and M. O. Ajewole, “Computational Analysis of Raindrop Radar Reflectivity and Radar Cross Section across Various Frequency Bands,” 2025, pp. 123–130. doi: 10.2991/978-94-6463-644-4_12.

[3] M. Lakkham, “Determining the appropriate altitude to improve accuracy in rainfall estimation from radar reflectivity data,” in *Journal of Physics: Conference Series*, Institute of Physics Publishing, Oct. 2017. doi: 10.1088/1742-6596/901/1/012045.

[4] E. Ghaemi, M. Gabella, U. Foelsche, I. Sideris, and D. Nerini, “The effect of altitude on the uncertainty of radar-based precipitation estimates over Switzerland,” *Int J Remote Sens*, vol. 44, no. 8, pp. 2495–2517, 2023, doi: 10.1080/01431161.2023.2203339.

[5] F. Simanjuntak, I. Jamaluddin, T. H. Lin, H. A. W. Siahaan, and Y. N. Chen, “Rainfall Forecast Using Machine Learning with High Spatiotemporal Satellite Imagery Every 10 Minutes,” *Remote Sens (Basel)*, vol. 14, no. 23, Dec. 2022, doi: 10.3390/rs14235950.

[6] V. Louf *et al.*, “An integrated approach to weather radar calibration and monitoring using ground clutter and satellite comparisons,” *J Atmos Ocean Technol*, vol. 36, no. 1, pp. 17–39, Jan. 2019, doi: 10.1175/JTECH-D-18-0007.1.

[7] M. De Biase *et al.*, “Integrated Rainfall Estimation Using Rain Gauges and Weather Radar: Implications for Rainfall-Induced Landslides,” *Remote Sens (Basel)*, vol. 17, no. 21, Nov. 2025, doi: 10.3390/rs17213629.

[8] J. Zhang, C. Langston, and K. Howard, “Brightband Identification Based on Vertical Profiles of Reflectivity from the WSR-88D,” *Journal of Atmospheric and Oceanic Technology - J ATMOS OCEAN TECHNOL*, vol. 25, Oct. 2008, doi: 10.1175/2008JTECHA1039.1.

[9] P. Chen, L. Chen, Q. Wu, G. Wang, and P. Zhang, “Analysis of Satellite-Ground Radar Reflectivity Consistency: First Evaluation Results of FY-3G and GPM Precipitation Radar,” *Geophys Res Lett*, vol. 52, no. 13, Jul. 2025, doi: 10.1029/2025GL115785.

[10] Y. Gou and H. Chen, “Combining radar attenuation and partial beam blockage corrections for improved quantitative application,” *J Hydrometeorol*, vol. 22, no. 1, pp. 139–153, 2020, doi: 10.1175/JHM-D-20-0121.1.

[11] A. D. Ochou, E.-P. Zahiri, B. Bamba, and M. Koffi, “Understanding the Variability of Z-R Relationships Caused by Natural Variations in Raindrop Size Distributions (DSD): Implication of Drop Size and Number,” *Atmospheric and Climate Sciences*, vol. 01, no. 03, pp. 147–164, 2011, doi: 10.4236/acs.2011.13017.

[12] J. I. Song, S. S. Yum, S. H. Park, K. H. Kim, K. J. Park, and S. W. Joo, "Climatology of Melting Layer Heights Estimated From Cloud Radar Observations at Various Locations," *Journal of Geophysical Research: Atmospheres*, vol. 126, no. 17, Sep. 2021, doi: 10.1029/2021JD034816.

[13] Z. Tan *et al.*, "Climatology of Cloud Base Height Retrieved from Long-Term Geostationary Satellite Observations," *Remote Sens (Basel)*, vol. 15, no. 13, Jul. 2023, doi: 10.3390/rs15133424.

[14] S. Chumchean, A. Seed, and A. Sharma, "Correcting of real-time radar rainfall bias using a Kalman filtering approach," *J Hydrol (Amst)*, vol. 317, no. 1–2, pp. 123–137, Feb. 2006, doi: 10.1016/j.jhydrol.2005.05.013.

[15] Y. A. Oh, H. L. Kim, and M. K. Suk, "Clutter elimination algorithm for non-precipitation echo of radar data considering meteorological and observational properties in polarimetric measurements," *Remote Sens (Basel)*, vol. 12, no. 22, pp. 1–18, Nov. 2020, doi: 10.3390/rs12223790.

[16] World Meteorological Organization, State of the Global Climate 2022, WMO-No. 1257. Geneva: World Meteorological Organization, 2023.

[17] Pramil, Prateek, and Parashuram, "Band Pass Semi Adaptive Digital Filters for Radar Applications," *Int J Eng Adv Technol*, vol. 9, no. 3, pp. 4184–4186, Feb. 2020, doi: 10.35940/ijeat.C5017.029320.

[18] C. Yoo, J. Yoon, J. Kim, and Y. Ro, "Evaluation of the gap filler radar as an implementation of the 1.5 km CAPPI data in Korea," *Meteorological Applications*, vol. 23, no. 1, pp. 76–88, Jan. 2016, doi: 10.1002/met.1531.

[19] D. S. Permana, T. D. F. Hutapea, A. S. Praja, F. Fatkhuroyan, and L. F. Muzayanah, "Pengolahan Dan Pemulihan Data Radar Cuaca Menggunakan Wradlib Berbasis Python," *Jurnal Meteorologi dan Geofisika*, vol. 17, no. 3, 2018, doi: 10.31172/jmg.v17i3.350.

[20] A. Overeem, H. DE VRIES, H. Al Sakka, R. Uijlenhoet, and H. Leijnse, "Rainfall-induced attenuation correction for two operational dual-polarization c-band radars in the Netherlands," *J Atmos Ocean Technol*, vol. 38, no. 6, pp. 1125–1142, Jun. 2021, doi: 10.1175/JTECH-D-20-0113.1.

[21] M. Heistermann, S. Jacobi, and T. Pfaff, "Technical Note: An open source library for processing weather radar data (wradlib)," *Hydrol Earth Syst Sci*, vol. 17, no. 2, pp. 863–871, 2013, doi: 10.5194/hess-17-863-2013.

[22] J. S. Marshall and W. McK. Palmer, "The distribution of raindrops with size," Journal of Meteorology, vol. 5, no. 4, pp. 165–166, 1948, doi: 10.1175/1520-0469(1948)005<0165:TDORWS>2.0.CO;2..

[23] N. A. Jamal, N. Mohamed Noor, I. A. M. Jafri, and G. J. Wibowo, "Assessment of Moving Average (MA) Method for Rainfall Prediction in Yogyakarta, Indonesia," MDPI AG, Mar. 2025, p. 5. doi: 10.3390/eesp2025033005.

[24] Q. Yan, B. Zhang, Y. Jiang, Y. Liu, B. Yang, and H. Wang, "Quality control of hourly rain gauge data based on radar and satellite multi-source data," *Journal of Hydroinformatics*, vol. 26, no. 5, pp. 1042–1058, May 2024, doi: 10.2166/hydro.2024.272.

[25] R. Villalobos-Herrera, S. Blenkinsop, S. B. Guerreiro, T. O'Hara, and H. J. Fowler, "Sub-hourly resolution quality control of rain-gauge data significantly improves regional sub-daily return level estimates," *Quarterly Journal of the Royal Meteorological Society*, vol. 148, no. 748, pp. 3252–3271, Oct. 2022, doi: 10.1002/qj.4357.

[26] M. Ding, Z. Shen, R. Huang, Y. Liu, and H. Wu, "Cross-Validation Methods for Multisource Precipitation Datasets over the Sparse-Gauge Region: Applicability and Uncertainty", doi: 10.1175/JHM-D-23.

[27] S. Ryu, J. J. Song, and G. W. Lee, "Radar–Rain Gauge Merging for High-Spatiotemporal-Resolution Rainfall Estimation Using Radial Basis Function Interpolation," *Remote Sens (Basel)*, vol. 17, no. 3, Feb. 2025, doi: 10.3390/rs17030530.

[28] N. S. Osman and W. Tahir, "Radar Quantitative Precipitation Estimation (QPE) Calibration Methods: A Systematic Literature Review," *Engineering, Technology and Applied Science Research*, vol. 14, no. 5, pp. 16185–16192, Oct. 2024, doi: 10.48084/etasr.7534.

[29] K. Dzwonkowski, I. Winnicki, S. Pietrek, and J. Siewert, "Analysis of Precipitation Totals Based on Radar and Rain Gauge Data," *Remote Sens (Basel)*, vol. 17, no. 13, Jul. 2025, doi: 10.3390/rs17132157.

EDUSJ, Vol, 35, No: 3, 2026 (95 - 105)

تحسين تقدير هطول الأمطار الراداري في يوجياكرتا باستخدام نـهج التصحيح الزمني واختيار الارتفاع القائم على نموذج الارتفاع الرقمي(DEM)

فرديناندو إدوين بينالون [1]، ألفين سياريف الدين سيهاب [2]

[1،2] محطة علم المناخ في يوجياكارتا، الوكالة الإندونيسية للأرصاد الجوية وعلم المناخ والجيوفيزياء

المستخلص

غالبًا ما تتأثر دقة التقدير الكمي لهطول الأمطار باستخدام الرادار بعدم اليقين في بيانات الانعكاسية الرأسية والاختلافات الزمنية مع القياسات السطحية .تهدف هذه الدراسة إلى تحديد الارتفاع الأمثل لأخذ العينات فوق سطح الأرض، ومواءمة الفارق الزمني بين بيانات رادار الطقس ومقاييس المطر التقليدية .تشمل الطرق المستخدمة ترشيحًا دقيقًا للبيانات الأولية متعددة الأحجام لتقليل التحيز، يليه استخراج الانعكاسية المحولة باستخدام علاقة مارشال-بالمر .Z-R يُظهر تحليل مفتاح الطور أن إزاحة زمنية عكسية بمقدار 10 دقائق) إزاحة زمنية (1- تُحقق أعلى ارتباط، مما يعكس مدة هطول الأمطار وتأخير المستشعر .أظهر التقييم الرأسي وجود توازن بين الدقة والاستقرار عند ارتفاع 600 متر، حيث تم الحصول على أقل متوسط لمتوسط الجذر التربيعي للخطأ 0.779) ملم(، وهو الأمثل للمناطق المنخفضة، على الرغم من ارتفاع مستوى عدم الاستقرار) انحراف معياري (0.493 نتيجة للتداخل في المناطق الجبلية .في المقابل، يُظهر ارتفاع 1400 متر أفضل استقرار للبيانات) انحراف معياري .(0.185 توصي هذه الدراسة بتطبيق تصحيح زمني بمقدار 10- دقائق واستخدام البيانات عند ارتفاعات تزيد عن 1200 متر كمنطقة مثلى لتقليل التشوه الطبوغرافي في المناطق ذات الخطوط الكنتورية الديناميكية.